

NMR linewidth, relaxation and diffusion studies of hexamethyldisilane confined in porous silica

Dagfinn W. Aksnes¹* and Liudvikas Kimtys²

¹ Department of Chemistry, University of Bergen, N-5007 Bergen, Norway

² Department of Physics, Vilnius University, Vilnius 2734, Lithuania

Received 23 March 1998; revised 18 May 1998; accepted 22 June 1998

ABSTRACT: The rotational and translational dynamics of hexamethyldisilane confined within silica pores of diameter 4, 6 and 20 nm were studied as a function of temperature by measuring ¹H and ¹³C NMR linewidths, self-diffusion coefficients, spin–spin relaxation times and spin–lattice relaxation times, and the results were compared with values obtained for the bulk material. The confinement in the pores gives rise to substantial changes in the molecular dynamics and phase behaviour. The lineshape, *T*₂ and self-diffusion measurements revealed a two-phase system consisting of a liquid-like component at the surface and a crystalline solid in the centre of the pore. The highly mobile surface layer is observable far below the reduced transition temperature of the confined hexamethyldisilane. A high diffusion rate of the adsorbed hexamethyldisilane is observed over a wide temperature range, even well below the region of the depressed transition point. The diffusion coefficient of the molecules in the surface layer is three orders of magnitude larger than in the plastic phase of bulk hexamethyldisilane. © 1998 John Wiley & Sons, Ltd.

KEYWORDS: porous silica; confined hexamethyldisilane; NMR spectroscopy; self-diffusion; relaxation

INTRODUCTION

NMR spectroscopy is a well established method for characterizing porous materials and for studying the phase behaviour and dynamics of fluids in confined geometry.¹ It is well known that a substance confined in pores exhibits different thermal and dynamic properties to the bulk material. Thus, when liquids are confined within small pores their freezing point temperature is reduced inversely with the mean pore diameter.² The geometric restrictions and surfaces have a large influence on both the translational and rotational behaviour of the confined molecules. In this respect, relaxation and diffusion studies give valuable information on pore geometries and on the important process of mass transport. By using organic molecules that form soft plastically crystalline phases on freezing as adsorbates, damage to the pore structures caused by ice formation can be avoided. Furthermore, the high translational mobility of plastic crystals compared with rigid crystals allows the direct determination of the self-diffusion coefficients using the pulsed-field gradient (PFG) NMR technique. However, these measurements are difficult owing to short spin–spin relaxation times *T*₂ which severely attenuate the measured signal even when the stimulated-echo technique is being used.

In the present work, hexamethyldisilane (HMDS) confined within silica gel pores of nominal diameter 4, 6 and 20 nm was studied by high-field NMR, and the results are discussed with reference to the bulk material. This is a model system which could provide useful information of both fundamental and practical interest. HMDS is expected to have a weak and non-specific interaction with silica but no freezing point depression data appear to be available. HMDS exhibits a disordered phase between the phase transition at 222 K and the melting point at 288 K.³ X-ray studies have established that the plastic phase (solid I) is body-centred cubic with two molecules per unit cell and a lattice constant, *a*, of 0.847 nm at 273 K³ and 0.843 nm at 225 K.⁴ The entropy of fusion is low compared with the entropy of transition: $\Delta S_f = 1.25$ R and $\Delta S_t = 5.25$ R.³

Previous NMR diffusion and radio-tracer measurements on HMDS have shown that the diffusion rate is relatively high in the plastic phase, making diffusion measurements feasible also in the confined systems. In an early ¹H linewidth study on HMDS,⁵ it was concluded, on the basis of the motionally averaged second moment, that the methyl reorientation (*C*₃ motion) is occurring at a faster rate than the molecular reorientation of the trimethylsilyl group about the Si–Si axis (*C*₃' motion) in solid II. Two later low-field ¹H relaxation studies (*T*₁ and *T*_{1ρ}) were based on the same assumption.^{6,7} However, a recent multinuclear NMR spin–lattice relaxation study on HMDS⁸ came to the opposite conclusion. In solid I, however, molecular tumbling and self-diffusion dominate the relaxation and line-narrowing processes.

Correspondence to: D. W. Aksnes, Department of Chemistry, University of Bergen, N-5007 Bergen, Norway. E-mail: dagfinn.aksnes@kj.uib.no
Contract/grant sponsor: Research Council of Norway.
Contract/grant sponsor: Lithuanian Academy of Science.
Contract/grant sponsor: Norwegian Academy of Science.

EXPERIMENTAL

Sample preparation

Three different commercial samples were used in this work. The first sample was Merck grade 10180, 70-230, with a nominal pore diameter of 4 nm, supplied by Aldrich. Its specific surface area was $750 \text{ m}^2 \text{ g}^{-1}$ and the specific pore volume was $0.68 \text{ cm}^3 \text{ g}^{-1}$. The second sample was Sorbsil C60-40/60, with a nominal pore diameter of 6 nm, supplied by Unilever. It had a specific surface area of $510 \text{ m}^2 \text{ g}^{-1}$ and a specific pore volume of $0.75 \text{ cm}^3 \text{ g}^{-1}$. The third sample was Sorbsil C200, with a nominal pore diameter of 20 nm, supplied by Unilever. It had a specific surface area of $299 \text{ m}^2 \text{ g}^{-1}$ and a specific pore volume of $1.70 \text{ cm}^3 \text{ g}^{-1}$. HMDS obtained from Aldrich (98%) was dried in molecular sieves and redistilled before use. The three test samples were prepared in 5 mm o.d. NMR tubes, each filled to a height of approximately 10 mm with porous silica gel. Physisorbed water was removed by drying the samples at 393 K in an oven for 12 h followed by evacuation at 0.3 Pa on a vacuum line. HMDS was then added to give a slight overfilling to the pores, the excess (<2%) going to fill the inter-granular space. The quantity to be added was calculated from the known specific pore volume of silica. In addition, a bulk sample of HMDS was prepared in a 2 mm o.d. NMR tube. The four NMR tubes were immediately sealed under vacuum to remove any dissolved oxygen and prevent evaporation and contamination. No measurable signals from impurities or physisorbed water were seen in the ^1H NMR spectrum of the investigated samples. Furthermore, under the high-resolution conditions used in this work, no background absorption from silanol species was seen.

NMR measurement procedures

The ^1H and ^{13}C measurements were carried out at 9.4 T on a Bruker DMX 400 WB spectrometer. The ^{13}C spectra were acquired with a high-resolution 5 mm probehead using a composite pulse decoupling power of ca 6 kHz. The self-diffusion measurements were performed with a Z-shielded 5 mm probehead producing 25 G A^{-1} . The field gradients were generated by the Bruker BAFPA 40 gradient unit ($G \leq 10 \text{ T m}^{-1}$). By applying gradient pre-emphasis with three-exponential correction terms the eddy current time after a gradient pulse was less than 300 μs . The strengths of the gradient pulses were calibrated indirectly by matching the measured self-diffusion constant of dried glycerine with the reported value ($1.73 \times 10^{-12} \text{ m}^2 \text{ s}^{-1}$ at 298 K).⁹ The 90° transmitter pulses were carefully calibrated (ca 6 μs) for all samples and temperatures. The sample temperature was regulated and stabilized to within $\pm 0.5 \text{ K}$ by means of a Bruker B-VT 2000 temperature-control unit. All the data presented were obtained by increasing the temperature after having cooled the samples to low

temperature initially to prevent the complication of undercooling or hysteresis. However, when a few measurements were made by cooling the samples no distinct hysteresis was seen.

The T_1 times were measured by standard inversion-recovery [$T-180^\circ-\tau-90^\circ\text{-FID}$], typically using 16 values of τ and the recycle delay $T \geq 5T_1$. The longest T_2 times ($\geq 0.7 \text{ ms}$) were measured using the CPMG sequence $T-90^\circ_x-[\tau-180^\circ_{\pm y}-\tau\text{-echo}]_n$ with $T \geq 5T_1$ and $\tau \ll T_2$ whereas the shorter T_2 values were estimated from the linewidths to avoid spin-locking effects for very short τ . The diffusion coefficients were measured using the stimulated spin-echo sequence [$T-90^\circ-\delta-t_r-90^\circ-\delta_s-\tau-90^\circ-\delta-t_r\text{-echo}$] where $T \geq 5T_1$, δ is the length of the gradient pulse, t_r is the ring-down time, δ_s is the gradient spoiler time and the gradient pulse spacing $\Delta = \delta + t_r + \delta_s + \tau$. The signal height of the Fourier transformed echo may be written $A = \text{constant} \times \exp[-\gamma^2 G^2 D \delta^2 (\Delta - \delta/3)]$, where G is the strength of the gradient pulses. The constant term contains a factor $\exp(-2\tau_1/T_2)$, where $\tau_1 = \delta + t_r$ ($\geq 1.3 \text{ ms}$ for the present measurements), which severely attenuates the measured echo for short spin-spin relaxation times T_2 . The estimated errors in T_1 , T_2 and the diffusion coefficient are within 5% with the exception of the short T_2 values evaluated from the overlapped linewidths.

RESULTS AND DISCUSSIONS

NMR lineshapes and linewidths

The ^1H lineshapes of bulk and confined HMDS at 160 K are shown in Fig. 1. The corresponding ^1H and ^{13}C linewidths, $\Delta\nu_{1/2}$ (full width at half-height) are shown in Figs 2 and 3. The extensive broadening of the ^{13}C resonances of HMDS in bulk and 20 nm pores in solid II is an artefact due to insufficient H decoupling power. The linewidth of the ^1H resonance of bulk HMDS in solid II

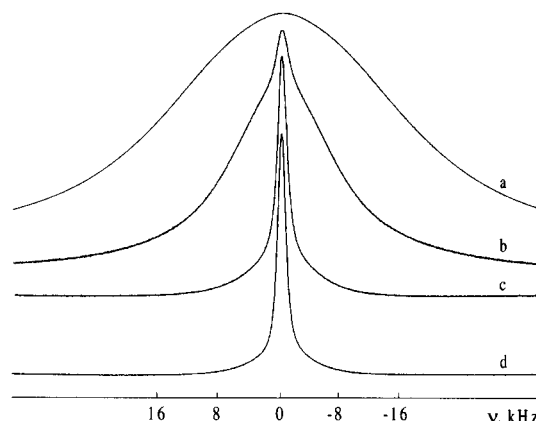


Figure 1. ^1H NMR lineshapes for bulk HMDS (a) and HMDS confined in silica with 20 nm (b), 6 nm (c) and 4 nm (d) pores at 160 K. The confined material shows a narrow-line component superimposed on a broad-line component.

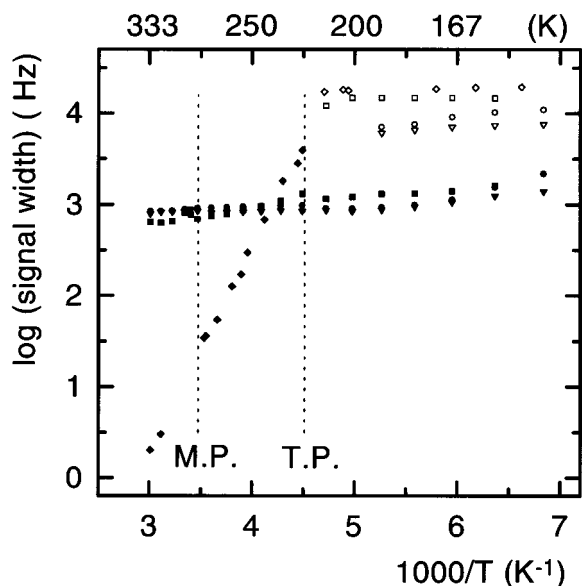


Figure 2. Temperature dependence of ^1H NMR linewidths for bulk HMDS (\diamond , \blacklozenge) and HMDS confined in silica with 20 nm (\square , \blacksquare), 6 nm (\circ , \bullet) and 4 nm (∇ , \blacktriangledown) pores. Open and filled symbols are used to distinguish between the broad and narrow signals, respectively. M.P. and T.P. indicate the melting and transition points of bulk HMDS.

(ca 19 kHz) is consistent with the value observed for *tert*-butyl protons narrowed by reorientations of the methyl and *tert*-butyl groups (C_3 and C_3' motions, respectively).^{10,11} The abrupt decrease in the ^1H and ^{13}C linewidths at the transition point of bulk HMDS is attributed to the onset of overall molecular tumbling in the plastic phase, whereas the additional ^1H line narrowing occurring with increasing temperature is caused

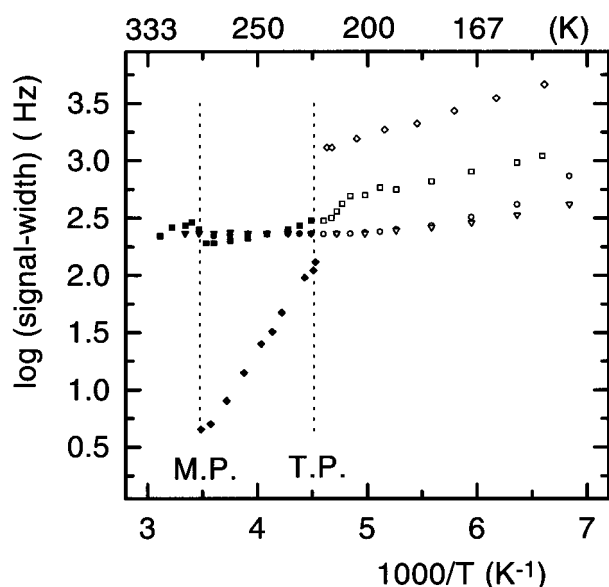


Figure 3. Temperature dependence of ^{13}C NMR linewidths for bulk HMDS (\diamond , \blacklozenge) and HMDS confined in silica with 20 nm (\square , \blacksquare), 6 nm (\circ , \bullet) and 4 nm (∇ , \blacktriangledown) pores. M.P. and T.P. indicate the melting and transition points of bulk HMDS.

by molecular self-diffusion. Linear regression on the ^1H and ^{13}C linewidth data yields activation energies of 42 and 28 kJ mol^{-1} for the translational and reorientational motions, respectively. The former value is in good agreement with the value obtained from our PFG self-diffusion data (43 kJ mol^{-1}).

The ^1H lineshape observations of HMDS confined within the 20 nm pores clearly revealed two distinct components below ca 220 K as demonstrated in Fig. 1. For the 6 and 4 nm pore systems the lineshapes also indicated, but not so clearly as for the larger pores, the presence of two components in the same temperature region. In the ^{13}C spectrum, however, we were not able to distinguish between the two components, probably because the two lines have comparable widths due to inhomogeneous line broadening (see below). The contribution of the narrow-line component in solid II, obtained with an accuracy of ca 10% from the ^1H data assuming Lorentzian lineshapes, decreases steadily from 100% at the transition point to ca 2.5, 31 and 60% at 157 K for the 20, 6 and 4 nm pore systems, respectively [Fig. 4(b)]. Since the narrowest component contributes 100% near the transition point and as much as ca 25% in the 20 nm pore system at 200 K, it cannot originate solely from the surface layer. The two-component system appearing in phase II is, therefore, a result of a significant pore size distribution of the silicas employed, attributed to a pore size-dependent depression of the solid–solid transition temperature. Hence, we believe that the narrow-line component observed in the solid II region largely corresponds to the undercooled disordered solid in the smaller pores and the broad-line component to the ordered solid in the larger pores.

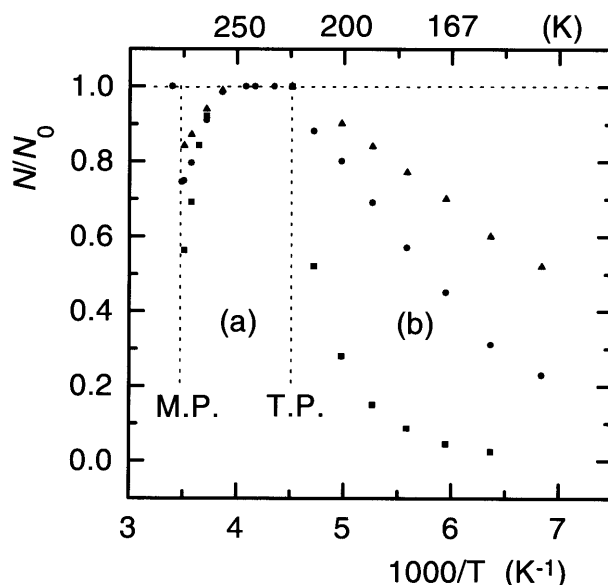


Figure 4. Temperature dependence of the relative contribution of the liquid-like narrow-line component of HMDS in 20 nm (\blacksquare), 6 nm (\bullet) and 4 nm (\blacktriangle) pores obtained from (a) PFG measurements in solid I and (b) lineshape measurements in solid II. M.P. and T.P. indicate the melting and transition points of bulk HMDS.

However, the excess bulk-like material in the intergranular space might give a small contribution to the broader signal. In the 6 and 4 nm systems the mobile surface layer is also expected to contribute significantly to the narrow signal, or even dominate the signal at the lowest temperatures, owing to the increased surface-to-volume ratio relative to the 20 nm pores by a factor of *ca* 4 and 6, respectively. This explains why the contribution of the narrow-line component increases with reduced pore size as shown in Fig. 4. In the 4 nm pores, for example, *ca* 50% of the molecules remain in the more mobile phase even 75 K below the bulk transition point.

The ^1H and ^{13}C resonances of confined HMDS in the liquid and solid I phases suffer a temperature-independent line broadening of approximately 2 ppm which is attributed to variations of the magnetic susceptibility in the sample.¹² This inhomogeneous line broadening prevents the observation of narrow resonances when the single-pulse experiment is used. Therefore, the present linewidth data apparently show a single component in contrast to the T_2 and self-diffusion measurements below which were based on the spin-echo sequence that eliminates any foreshortening of transverse relaxation due to magnetic field inhomogeneities.

Spin-spin relaxation

The T_2 values for bulk and confined HMDS are shown as semi-logarithmic plots versus the reciprocal of temperature in Fig. 5. Owing to spin-locking effects only T_2 values longer than 0.7 ms were measured with the

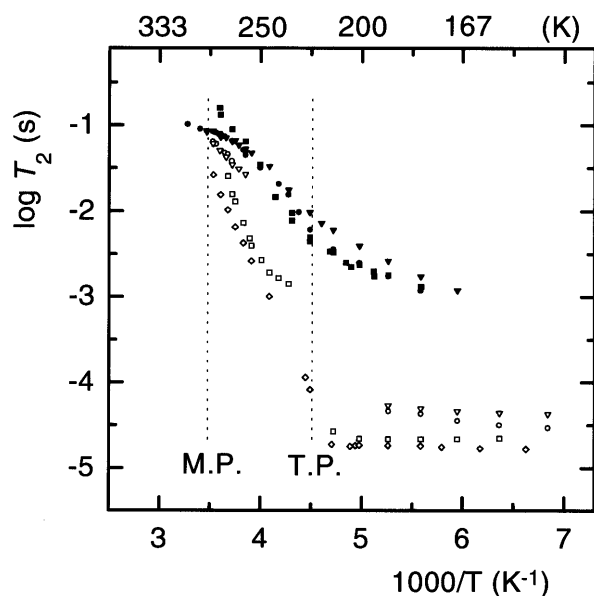


Figure 5. Temperature dependence of T_2 for bulk HMDS (\diamond) and HMDS confined in silica with 20 nm (\square , \blacksquare), 6 nm (\circ , \bullet) and 4 nm (∇ , \blacktriangledown) pores. Open and filled symbols are used to distinguish between the broad and narrow signals, respectively. M.P. and T.P. indicate the melting and transition points of bulk HMDS.

CPMG spin-echo sequence, whereas the shorter T_2 values were evaluated from the linewidths according to the relationship

$$T_2 = \frac{1}{\pi \Delta\nu_{1/2}} \quad (1)$$

The discontinuous increase in T_2 of bulk HMDS from 19 μs at 223 K to 82 μs at 213 K is associated with a structural phase transition from an ordered phase where only anisotropic C_3 and C_3' reorientations take place to a plastic face-centred cubic structure allowing overall molecular tumbling and translational diffusion. Two relatively narrow components of confined HMDS appear in the temperature region between the melting and transition points of the bulk material. The T_2 of the broader component was measurable down to *ca* 234 K for the 20 nm pore system but only down to *ca* 260 K for the smaller pore systems. Note that the inhomogeneous line broadening prevents separation of the two narrow components with different T_2 when the single-pulse sequence is used (see Experimental). The more narrow component is attributed to the liquid-like component at the surface of the pores whereas the other component is assigned to the plastic phase at the interior of the pores in agreement with conclusions made for cyclohexane.¹³⁻¹⁵ In the freezing region, the liquid in the smaller pores that remains unfrozen will also contribute to the narrow signal. The relative distribution of the two components, obtained from the self-diffusion measurements, will be explained in the next section [Fig. 4 (a)].

The general trend is a small increase in T_2 of both components with reduced pore size throughout the solid I and II regions, in agreement with observations made for confined cyclohexane.^{13,14} It is also seen that T_2 of the broad-line component is consistently longer than that for the bulk material. However, the T_2 behaviour of the broad-line component in the 20 nm pores is not significantly different from that for the bulk material. This is reasonable since the broad component is thought to originate from the bulk-like crystals at the centre of the pores. In solid II, the T_2 (linewidth) of both the bulk and 20 nm samples becomes independent of temperature above 150 K, reaching plateaux of 17 and 22 μs , respectively. This indicates that the partial averaging of the nuclear dipole-dipole interaction by the C_3 and C_3' motions is complete. For HMDS in 6 and 4 nm pores, the contribution of the broad component is much lower owing to the increased surface-to-volume ratio by a factor of *ca* 4 and 6, respectively, as explained in the previous section [Fig. 4 (b)]. Here, the line narrowing caused by the anisotropic motions appears to be complete at 146 K, yielding a value of T_2 of 29–42 μs . However, owing to rather inaccurate T_2 values, evaluated from the linewidths, in this temperature region we cannot conclude that the reorientational motion is occurring at a faster rate than in the bulk material. Clear evidence for a solid-solid phase transition from the plastic to the brittle phase is also seen for the broad component of all confined samples, in contrast to obser-

vations made for cyclohexane confined within silicas obtained from the same source.¹⁴

T_2 of the narrow-line component appears to be continuous across the melting and transition points, decreasing uniformly from 82–220 ms at the melting point, depending on pore size, to approximately 1.3 ms for all pore sizes at 179 K. The transverse relaxation times of confined cyclohexane are also relatively long even far below the transition point,^{13,14} whereas other liquids forming ordinary crystals such as water and tetradecane¹⁶ show a much faster change of T_2 with decreasing temperature. These observations suggest that persistent highly mobile surface layers exist throughout the temperature region of the bulk plastic phase and far into the ordered phase of confined HMDS and cyclohexane.

In the two-component region we must consider the mobility of molecules between the two regions. Over the time of the experiment, t ($\sim T_2$), a molecule may travel a distance of the order of $\sqrt{6Dt}$. At 272 K, the highest temperature at which two T_2 components are clearly seen for the 20 nm sample in the solid I region, $T_2 = 25$ ms and $D = 1.2 \times 10^{-13} \text{ m}^2 \text{ s}^{-1}$ (see next section) for the slowly diffusing component at the centre of the pore. Thus, a molecule at the interior of the pore may travel approximately 134 nm over the time of the experiment. This should allow averaging of molecules at the interior of the pore with short T_2 into the longer T_2 component at the pore walls. However, in this temperature region the rapidly diffusing molecules originate largely from the liquid in the smaller pores that remains unfrozen, whereas the slowly diffusing molecules are attributed to the plastically crystalline phase in the larger pores. The observation of two distinct components in all confined systems, however, implies slow exchange ($\tau_{\text{ex}} > T_2$) between the different pore regions. Below the melting region the rapidly diffusing component, observed for all confined samples, is due solely to the mobile surface layer. However, T_2 of the slowly diffusing component at the interior of the pore was only measurable for the 20 nm sample below the melting region in solid I. Below the melting region of the 20 nm sample at, say, 250 K a molecule at the centre of the pore may travel approximately 12 nm over the time of the experiment. This should allow averaging between molecules residing at the pore walls and those at the interior of the pore, in disagreement with experiment since two distinct components are seen. Hence this observation implies slow exchange on the T_2 time-scale of molecules between the two regions within the same pore, possibly because the molecules at the pore walls are weakly attached to the surface.

Self-diffusion

We also measured the self-diffusion coefficients of bulk HMDS in the liquid and plastic phases using the PFG technique and compared the results with reported values based on radiotracer and $T_{1\rho}$ measurements⁷

(Fig. 6). An exact agreement between the results obtained from the different types of measurement is not expected owing to correlation effects which depend on the diffusion mechanism and the lattice structure of the solid.¹⁰ However, the anomalously high diffusion coefficients close to the melting point measured by the radiotracer technique are deemed to be imprecise owing to the high volatility of the solid.¹⁷ The diffusion coefficient of bulk HMDS undergoes a discontinuous change of more than three orders of magnitude at the melting point from $9.3 \times 10^{-10} \text{ m}^2 \text{ s}^{-1}$ in the liquid to $5.4 \times 10^{-13} \text{ m}^2 \text{ s}^{-1}$ in the plastic phase. The corresponding activation energy increases from 15 to 43 kJ mol⁻¹. The latter value agrees well with our linewidth data (42 kJ mol⁻¹) and previous $T_{1\rho}$ measurements by Chadwick *et al.*⁷ (44 kJ mol⁻¹) but deviates considerably from the value obtained from radiotracer measurements by the same authors⁷ (52 kJ mol⁻¹) and from radiotracer and plastic deformation measurements by Salthouse and Sherwood¹⁸ (71 and 68 kJ mol⁻¹, respectively). This is in accord with previous observations that the activation energy for the line-narrowing process of low entropy of fusion solids (< 2.5 R) is much lower than that obtained from plastic deformation and radiotracer measurements.^{10,18}

The mean interval between consecutive jumps, τ , can be obtained from T_2 using Torrey's isotropic random-walk model:^{10,19,20}

$$\frac{1}{T_2} = 0.955 M_{2r} \tau \quad (2)$$

where M_{2r} is the rotationally averaged second moment. The mean value of M_{2r} evaluated from low-field $T_{1\rho}$ measurements is $3.11 \times 10^8 \text{ s}^{-2}$.⁷ The average time

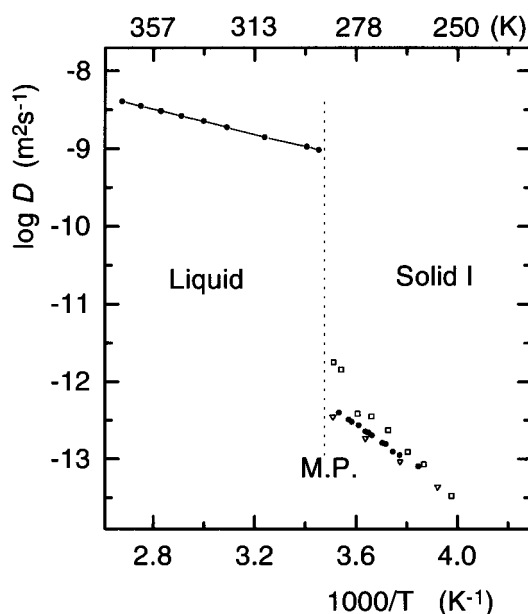


Figure 6. Temperature dependence of the self-diffusion coefficient of bulk HMDS obtained from PFG measurements (●) and radiotracer measurements (□) and evaluated from $T_{1\rho}$ measurements (▽).

between diffusional jumps at the melting point is thus calculated to be 1.0×10^{-7} s, in good agreement with the average value reported for other body-centred cubic solids, $(1.2 \pm 0.6) \times 10^{-7}$ s.¹⁰

An average value of 0.63 nm is evaluated for the mean square jump distance over the temperature range studied in this work by using the τ values evaluated from Eqn (2) and the Einstein relationship:

$$\langle r^2 \rangle = 6D\tau \quad (3)$$

This value is in reasonable agreement with the nearest neighbour distance in the HMDS lattice at 273 K (0.73 nm),³ indicating that molecular flights largely go to the nearest neighbour sites.

In Fig. 7, the measured self-diffusion coefficients of confined HMDS, presented as semi-logarithmic plots versus reciprocal of temperature, are compared with the values obtained for the bulk material. The stimulated echo signal contained both a rapidly diffusing and a slowly diffusing component. By varying the strength of the magnetic field gradient from zero to a maximum value of 10 T m^{-1} we were able to separate and evaluate the relative contributions of the two components [Fig. 4 (a)]. On the time-scale of our experiment (*ca.* 10 ms), the molecules in the rapidly diffusing component in the solid I region will migrate over a region that exceeds the mean pore diameter by one to two orders of magnitude. Hence, the narrow component is attributed to both the rapidly diffusing molecules in the mobile layer at the pore walls and the liquid in the smaller pores that remains unfrozen, whereas the plastic component at the

interior of the larger pores gives rise to the slowly diffusing signal. The apparent contribution of the rapidly diffusing component increases from approximately 50–80% near the melting point, depending on pore size, to 100% at 250 K. This observation reflects a steadily decreasing signal contribution from the slowly diffusing molecules at the interior of the pores with decreasing temperature when T_2 becomes comparable to $2\tau_1$ (see Experimental). It follows that we only observe the spin-echo signal, and therefore the diffusion coefficient, of the mobile molecules at the pore walls below 250 K. The absolute contribution of the rapidly diffusing component was not measured quantitatively owing to the T_2 dependence mentioned above, but the signal appeared to decrease as more and more of the liquid in the smaller pores froze.

For all pore sizes the diffusion rate of the slowly diffusing molecules is comparable to that of bulk HMDS, confirming that the signal originates from the crystalline solid in the interior of the pores. The rapidly diffusing component, possessing a diffusion coefficient that is continuous across the melting and transition points, appears to be a continuation of the liquid behaviour, in agreement with observations made for T_2 . The slight curvature of the diffusion curve near the melting point might indicate that the contribution from the slowly diffusion components has not been completely removed, in particular for the 20 nm pore system. A high diffusion rate of the liquid-like molecules at the pore walls is observed over a wide temperature range, even far below the transition point of the bulk material.^{14,21} Indeed, the observed D values are more than three orders of magnitude larger than in the plastic phase of bulk HMDS, reflecting fast diffusion of persistent mobile molecules at the surface layer. A slight increase in the measured diffusion coefficient with reduced pore size (increased surface-to-volume ratio) is apparent. The apparent activation energy, obtained from the linear region of the slope, is in the range 20–22 kJ mol⁻¹ for the surface component, that is, approximately half the value observed for the molecules at the interior of the pores (45–51 kJ mol⁻¹).

Spin-lattice relaxation

Semi-logarithmic plots of the ^1H and ^{13}C T_1 values of bulk and confined HMDS versus inverse temperature are shown in Figs 8 and 9. The negative slopes of the T_1 curves show that all T_1 values are on the high-temperature side of the minimum, hence the extreme narrowing condition prevails. The ^{13}C T_1 of the bulk material, which is believed to be dominated by intramolecular relaxation modulated by the composite motion of the CH_3 group²² (overall tumbling and internal rotations) in the liquid and solid I phases, is continuous across the melting point, whereas the activation energy decreases from 7.1 kJ mol⁻¹ in solid I to 5.8 kJ mol⁻¹ in the liquid. By contrast, the ^1H T_1 curve of the bulk material shows a marked discontinuity at the

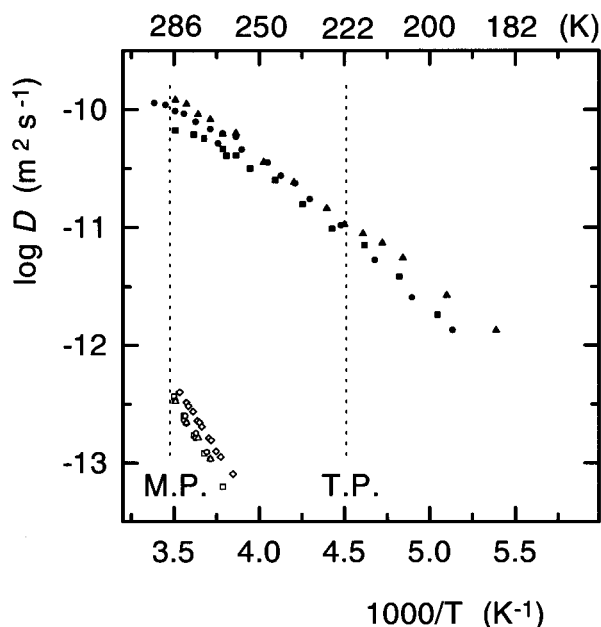


Figure 7. Temperature dependence of the self-diffusion coefficient for bulk HMDS (\diamond) and HMDS confined in silica with 20 nm (\square , \blacksquare), 6 nm (\circ , \bullet) and 4 nm (∇ , \blacktriangledown) pores. Open and filled symbols are used to distinguish between the broad and narrow signals, respectively. M.P. and T.P. indicate the melting and transition points of bulk HMDS.

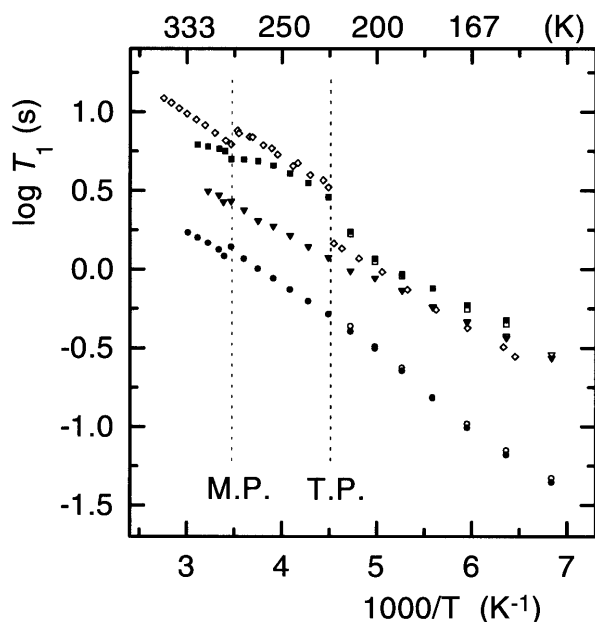


Figure 8. Temperature dependence of ^1H T_1 for bulk HMDS (\diamond) and HMDS confined in silica with 20 nm (\square , \blacksquare), 6 nm (\circ , \bullet) and 4 nm (∇ , \blacktriangledown) pores. Open and filled symbols are used to distinguish between the broad and narrow signals, respectively. M.P. and T.P. indicate the melting and transition points of bulk HMDS.

melting point, while the corresponding activation energy increases from 7.0 kJ mol^{-1} in solid I to 7.9 kJ mol^{-1} in the liquid. The essentially identical activation energy obtained from the ^1H and ^{13}C data in solid I is a

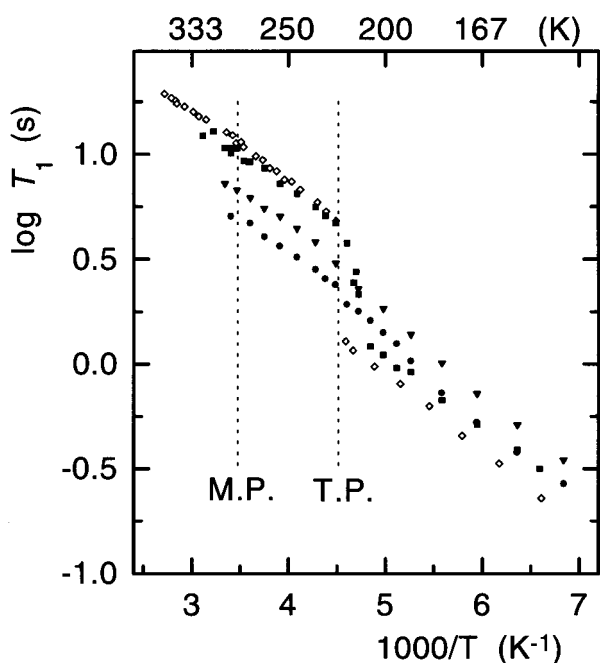


Figure 9. Temperature dependence of ^{13}C T_1 for bulk HMDS (\diamond) and HMDS confined in silica with 20 nm (\blacksquare), 6 nm (\bullet) and 4 nm (\blacktriangledown) pores. M.P. and T.P. indicate the melting and transition points of bulk HMDS.

poor measure for the overall molecular tumbling since it reflects the composite motion of the methyl groups. Furthermore, the contribution to ^1H T_1 from the intermolecular relaxation mechanism modulated largely by translational diffusion is significant in the liquid state. However, a reasonable activation energy of 28 kJ mol^{-1} for the overall tumbling was obtained from the ^{13}C line-width data.

The large discontinuity in the ^1H and ^{13}C T_1 values of bulk HMDS at the transition point is associated with a structural change of phase from a disordered solid allowing overall molecular tumbling to an ordered solid where only anisotropic molecular reorientations occur. Since T_1 increases linearly with temperature on the semi-logarithmic plots (Figs 8 and 9), a single reorientational process appears to be controlling T_1 in solid II. However, in two earlier low-field studies^{6,7} a maximum was observed for ^1H T_1 with increasing temperature due to the onset of a new motional process, believed to be C_3 reorientations,⁸ with activation energy $30\text{--}31 \text{ kJ mol}^{-1}$.^{6,7} Since this maximum is shifted to higher temperature with increasing field strength, it is not observed at 400 MHz before the phase transition intervenes. The activation energies obtained from our ^1H and ^{13}C T_1 data are identical within experimental error (7.1 and 7.0 kJ mol^{-1} , respectively) indicating that the same anisotropic motion, assigned to the C_3' rotation about the Si—Si axis, is controlling the relaxation of both nuclei in solid II.⁸ However, T_2 , being more sensitive to slower motions than T_1 , is affected by both the C_3 and C_3' motions.

Interestingly, the ^1H T_1 values measured for the narrow-line and broad-line components below the phase transition temperature (222 K) are identical within experimental error for all confined systems (Fig. 8), in contrast to the T_2 values which are very different for the two components. This implies that the fast exchange limit is fulfilled for T_1 , but not T_2 , in confined HMDS. Hence, only a single T_1 , averaged over the adsorbed and crystalline phases, is observed. It follows that the exchange time of HMDS confined within, for example, the 6 nm pores is between the limits $5 \text{ ms} < \tau_{\text{ex}} < 500 \text{ ms}$ at 222 K. Since the inhomogeneous line-broadening prevents observation of resonances more narrow than $\text{ca } 800 \text{ Hz}$, it is not possible to measure directly T_1 of the individual narrow-line components in the solid I and liquid phases. However, again, the observed T_1 will be an averaged value over the two components.

The ^1H and ^{13}C T_1 behaviour of HMDS confined in the 20 nm pores is not significantly different from that of the bulk material in solid II and the low-temperature region of solid I. As the melting point is approached, however, the ^1H T_1 curve levels off and appears to be approaching a maximum in the melting region, indicating an increasing contribution from the intermolecular relaxation mechanism governed by translation diffusion in the bulk-like liquid at the interior of the pores as more and more of the confined molecules melt. A corresponding levelling off in ^1H T_1 of the 6 and 4 nm

samples is not seen, however, possibly because the diffusion of the adsorbed molecules at the surface (which account for most or a dominant part of the confined molecules) is more restricted than for the bulk-like liquid molecules at the centre of the large 20 nm pores.¹⁴ Indeed, when HMDS is confined within the smaller pores T_1 of both nuclei is considerably reduced in the liquid and solid I phases again presumably owing to more restricted reorientational and translational motions. This is in accord with observations made in the corresponding confined cyclohexane systems which show that ^1H T_1 decreases with reduced pore size.¹⁴ It is difficult, however, to understand why T_1 of HMDS confined in the 4 nm pores is intermediate between the values measured in 20 and 6 nm pores, since this discrepancy is not seen in the T_2 results or for the cyclohexane systems.¹⁴ At the transition point, for example, ^1H T_1 is reduced from 3.3 s in the bulk sample to 2.9 s in 20 nm silica, 0.5 s in 6 nm silica and 1.2 s in 40 nm silica. In solid II, only T_1 of the methyl protons in the 6 nm sample deviates significantly from the value in the bulk material, whereas the effect of the confinement on T_1 of the methyl carbons appears to be reversed in the smaller pores.

The marked discontinuities seen for ^1H T_1 in all samples at the melting point indicate that the intermolecular relaxation mechanism is becoming more important in the liquid phase even for the smaller pore systems. The T_1 curves of both the ^1H and ^{13}C nuclei show clear evidence for a phase transition near 222 K in the bulk and 20 nm samples but not for the smaller pore sizes, in accord with observations made for confined cyclohexane.¹⁴ The present T_2 measurements, however, demonstrate a solid–solid phase transition for all the three confined samples.

Acknowledgements

We are indebted to the Research Council of Norway and the Lithuanian and Norwegian Academies of Science for providing support to carry out this research.

REFERENCES

1. P. J. Barrie, *Annu. Rep. NMR Spectrosc.* **30**, 37 (1995).
2. C. L. Jackson and G. B. McKenna, *J. Chem. Phys.* **93**, 9002 (1990).
3. H. Suga and S. Seki, *Bull. Chem. Soc. Jpn.* **32**, 1088 (1959).
4. J. P. Amoureux, M. Foulon, M. Muller and M. Bee, *Acta Crystallogr., Ser. B* **42**, 78 (1986).
5. T. Yukitoshi, H. Suga, S. Seki and J. Itoh, *J. Phys. Soc. Jpn.* **12**, 506 (1957).
6. S. Albert, H. S. Gutowsky and J. A. Ripmeester, *J. Chem. Phys.* **56**, 1332 (1972).
7. A. V. Chadwick, J. M. Chezeau, R. Folland, J. W. Forrest and J. H. Strange, *J. Chem. Soc., Faraday Trans. 1* **1610** (1975).
8. D. W. Aksnes and L. Kimtys, *Acta Chem. Scand.* **49**, 722 (1995).
9. M. I. Hrovat and C. G. Wade, *J. Magn. Reson.* **44**, 62 (1981).
10. J. N. Sherwood (Ed.), *The Plastically Crystalline State*. Wiley, New York (1979).
11. N. G. Parsonage and L. A. K. Staveley, *Disorder in Crystals*. Clarendon Press, Oxford (1978).
12. A. T. Watson and C. T. P. Chang, *Prog. Nucl. Magn. Reson. Spectrosc.* **31**, 343 (1997).
13. H. F. Booth and J. H. Strange, *Mol. Phys.* **93**, 263 (1998).
14. D. W. Aksnes and L. Gjerdåker, *J. Mol. Struct.* in press.
15. S. Stapf, R. Kimmich and T. Zavada, *Appl. Magn. Reson.* **12**, 199 (1997).
16. S. Stapf and R. Kimmich, *J. Chem. Phys.* **103**, 2247 (1995).
17. P. Bladon, N. C. Lockhart and J. N. Sherwood, *Mol. Phys.* **20**, 577 (1971).
18. P. W. Salthouse and J. N. Sherwood, *J. Chem. Soc., Faraday Trans. 1* **1845** (1977).
19. H. C. Torrey, *Phys. Rev.* **92**, 962 (1953).
20. H. C. Torrey, *Phys. Rev.* **96**, 690 (1954).
21. D. W. Aksnes, L. Gjerdåker, S. G. Allen, H. F. Booth and J. H. Strange, *Magn. Reson. Imaging* in press.
22. D. W. Aksnes and L. Kimtys, *Magn. Reson. Chem.* **28**, S20 (1990).